Cancer Immunology, Immunotherapy (2025) 74:22
https://doi.org/10.1007/s00262-024-03865-5

RESEARCH

Periodontitis promotes tumor growth and immune evasion via PD-1/PD-L1

Suli Wang[1] · Fujiao Nie[1] · Qiuyue Yin[1] · Haoyang Tian[1] · Pizhang Gong[1] · Jinhong Ju[1] · Jiayi Liu[1] · Pishan Yang[1] · Chengzhe Yang[2]

Received: 31 August 2024 / Accepted: 16 October 2024

Abstract

Background Our study investigated the role of experimental periodontitis on tumor growth, local and systemic immunosuppressive status, and programmed death receptor 1 (PD-1) / programmed death ligand 1 (PD-L1) expression in oral squamous cell carcinoma (OSCC) and prostate cancer.

Methods Mouse oral or prostate cancer xenograft models were divided into control, periodontitis and periodontitis + anti-PD-1 groups. Tumor volume and weight were recorded and the levels of relevant immune-suppressive cells and T cells were detected by flow cytometry or immunofluorescence. THP-1 cells were stimulated using conditioned media of LPS-stimulated Cal-27 cells and PD-L1 expression was measured by quantitative real-time PCR, western blotting and immunofluorescence. Tumor specimens from OSCC patients with or without periodontitis were also collected for immunofluorescence.

Results Periodontitis significantly promoted tumor volume and weight. Compared to the control, the proportions of tumor-associated macrophages (TAMs), regulatory T cells (Tregs), PD-L1$^+$TAMs and PD-1$^+$CD8$^+$T cells increased, while CD8$^+$T cells decreased in the periodontitis group. Immunofluorescence demonstrated that there was an increase in PD-L1$^+$TAMs and PD-1$^+$CD8$^+$T cells, but a decrease in IFN-γ^+CD8$^+$T cells in both xenografts and clinical OSCC samples with periodontitis. In vitro, LPS-stimulated Cal-27 cells had a stronger potential to induce PD-L1 expression in macrophages compared with unstimulated Cal-27 cells. And the promoting effect of periodontitis on tumor growth and immune evasion was significantly attenuated after anti-PD-1 therapy.

Conclusion Periodontitis may facilitate tumor growth and immune escape evidenced by the increased immune-suppressive cells and the decreased functional T cells, via enhancing PD-1/PD-L1 expression in the tumor microenvironment.

Keywords Periodontitis · Oral cancer · Prostate cancer · Tumor immunosuppression microenvironment · PD-1/PD-L1

Abbreviations

3D	Three-dimensional
BHI	Brain heart infusion
CFU	Colony-forming units
CM	Conditioned media
CMC	Carboxymethylcellulose
DAPI	4',6-Diamidino-2-phenylindole
FcγRs	Fcγ-receptors
FISH	Fluorescence in situ hybridization
Fn	*Fusobacterium nucleatum*
GAPDH	Glyceraldehyde-3-phosphate dehydrogenase
HE	Hematoxylin and eosin
IF	Immunofluorescence
IHC	Immunohistochemistry
IL	Interleukin
IL1R1	IL-1 receptor type 1
iTME	Immunosuppressive tumor microenvironment

✉ Pishan Yang
yangps@sdu.edu.cn

✉ Chengzhe Yang
yangchengzhe@email.sdu.edu.cn

[1] Department of Periodontology, School and Hospital of Stomatology, Cheeloo College of Medicine, Shandong University & Shandong Key Laboratory of Oral Tissue Regeneration & Shandong Engineering Research Center of Dental Materials and Oral Tissue Regeneration & Shandong Provincial Clinical Research Center for Oral Diseases, No. 44-1 Wenhua Road West, 250012 Jinan, Shandong, China

[2] Department of Oral and Maxillofacial Surgery, Qilu Hospital of Shandong University, No. 107 Wenhua Road West, 250012 Jinan, Shandong, China

Published online: 13 November 2024

MDSCs	Myeloid-derived suppressor cells
Micro-CT	Micro-Computed Tomography
OSCC	Oral squamous cell carcinoma
PD-1	Programmed death receptor 1
PD-L1	Programmed death ligand 1
Pg	*Porphyromonas gingivalis*
PMA	Phorbol 12-myristate 13-acetate
qRT-PCR	Quantitative real-time Polymerase Chain Reaction
SD	Standard deviation
TAMs	Tumor-associated macrophages
TGF-β	Transforming growth factor-β
TME	Tumor microenvironment
TNF-α	Tumor necrosis factor-α
Tregs	Regulatory T cells
WB	Western blotting

Introduction

In recent years, tumor immunity has received increasing attention. During tumorigenesis and development, the tumor evades immune surveillance characterized by an accumulation in functionally exhausted T cells as well as Tregs through a variety of mechanisms [1]. There are two primary pathways that have been elucidated: immunosuppression resulting from modifications to genes in tumor cells and adaptive resistance mediated by T cells. In the former, gene alterations in tumor cells mediate immunosuppression in three main ways: the secretion of immunosuppressive molecules including interleukin (IL)-10, IL-6 and transforming growth factor-β (TGF-β); the generation of immune-suppressive cells such as tumor-associated macrophages (TAMs), regulatory T cells (Tregs) and myeloid-derived suppressor cells (MDSCs); and the intrinsic upregulation of suppressive immune checkpoint molecules like programmed death receptor 1 (PD-1) and programmed death ligand 1 (PD-L1) [2, 3]. Additionally, local and systemic inflammatory microenvironment also contributes to immunosuppressive tumor microenvironment (iTME) [1, 4].

Periodontitis is a systemic chronic low-grade inflammation [5]. The relationship between periodontitis and cancers, including those of oral cavity and prostate has long been of interest and patients with periodontitis have an increased risk of cancers [6]. And effective therapy for periodontitis may potentially decrease the susceptibility to cancer [7]. Periodontal pathogens, such as *Fusobacterium nucleatum (Fn)* and *porphyromonas gingivalis (Pg)* facilitate the advancement of tumors including oral, colorectal and prostate cancers through different mechanisms [8–10] and *Pg* up-regulates PD-L1 expression in prostate cancer cells [10]. Moreover, Shi et al. revealed that experimental periodontitis could facilitate colorectal cancer progression and immunosuppressive microenvironment [11]. However, the effect of periodontitis as a disease entity on tumor immunity in other tumors remains largely unclear.

Therefore, this work further explored the effect of periodontitis on tumor progression and immune microenvironment in oral and prostate cancers, and probed the mediation role of PD-1/PD-L1. We wish that our findings could shed light on the underlying mechanisms linking periodontitis and oral cancer, laying a theoretical framework for improving iTME through the treatment of periodontitis [12].

Materials and methods

Cell and bacterial culture

Human monocyte cell line THP-1, human oral squamous cell carcinoma cell line Cal-27, mouse prostate cancer cell line RM-1 and mouse squamous cell carcinoma cell line SCC7 (all obtained from the Cell Bank of Chinese Academy of Science, Shanghai, China) were cultivated in DMEM (Vivacell, China) or RPMI 1640 (Vivacell, China) media. All the cells were maintained in a humidified growth chamber with 5% CO2 at a temperature of 37 °C.

Fn strain (ATCC 25586) was supplied by the Shandong Key Laboratory of Oral Tissue Regeneration (Jinan, China) and was grown in brain heart infusion (BHI) broth with hemin (5 mg/l) and Vitamin K1 (1 mg/l) at 37 °C in anaerobic conditions.

Animal model establishment

Five-week-old C57BL/6 J and C3H/He male mice were obtained from Beijing Vital River Laboratory Animal Technology Co., Ltd. (Beijing, China) and grown under SPF conditions. The mice were randomized into 3 groups: (1) Control group, only xenograft; (2) EP group, xenograft plus periodontitis; (3) EP + Anti-PD-1 group, same as EP group plus anti-PD-1 therapy. All mice in the experimental periodontitis group were anesthetized by intraperitoneal injection of 1% pentobarbital, and 5–0 silk ligatures were tied to the maxillary second molars bilaterally [13]. 2% carboxymethylcellulose (CMC) solution containing 10^9 colony-forming units (CFU) *Fn* was placed on the ligatures for 3 consecutive days following the ligation. The ligatures were checked every 3 days and religated if necessary, and were maintained throughout the experimental period. For the xenograft model, the mice were subcutaneously inoculated with 5×10^5 SCC7 cells or 3×10^5 RM-1 cells. For anti-PD-1 therapy, anti-PD-1 antibody (clone RMP1-14, BioXCell) (200 μg/mouse) was injected intraperitoneally on days 10, 13, 16, 19 and 22 after tumor inoculation. Tumor size was measured every 3 days and calculated using the formula

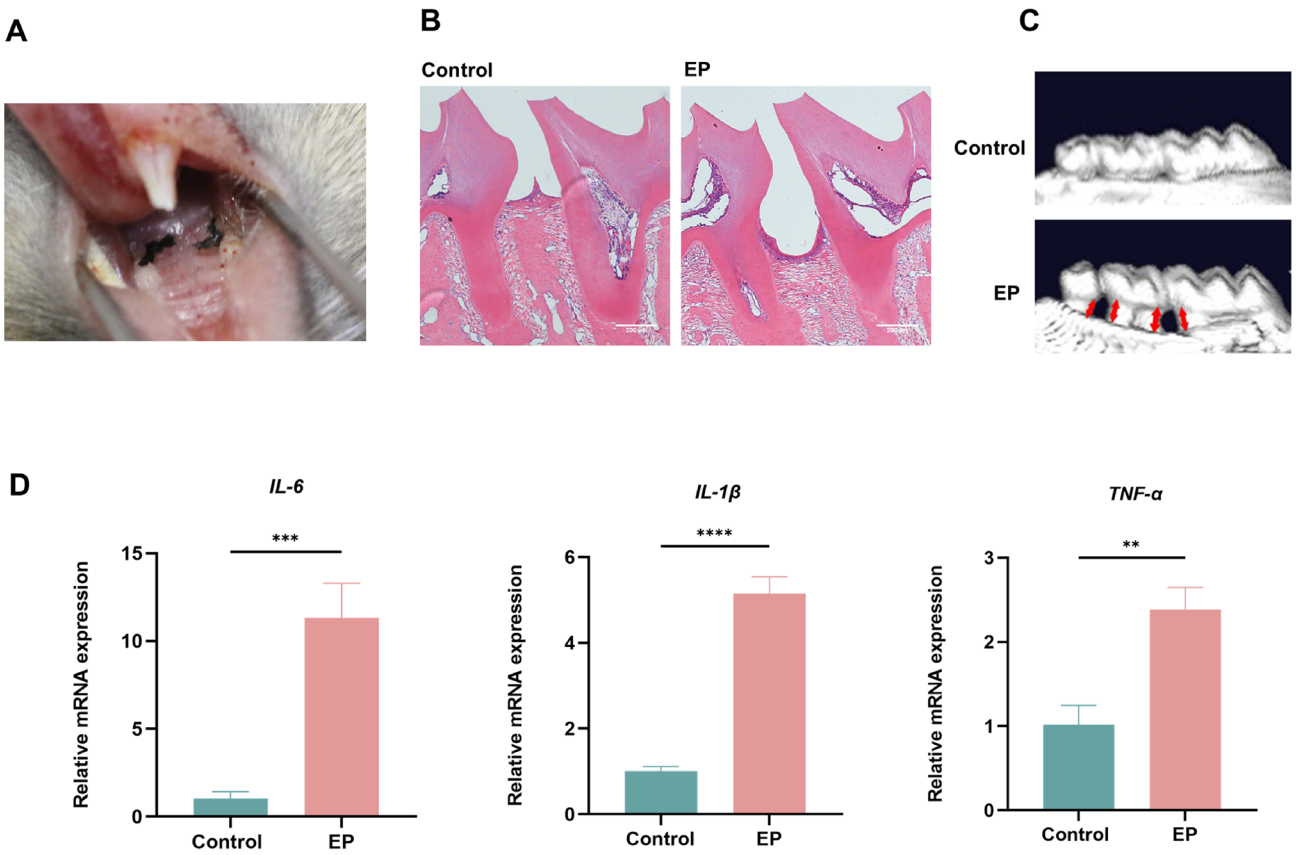

Fig. 1 Modeling of an experimental periodontitis. **A** Induction of periodontitis by silk ligation of the bilateral maxillary second molars in mice. **B** HE staining of the control and experimental periodontitis groups. **C** 3D reconstructed images of alveolar bone in each group. The red arrows represent the distance from the cementoenamel junction to the alveolar bone crest (CEJ-ABC). **D** IL-6, IL-1β and TNF-α mRNA levels of gingival tissues in each group measured by qRT-PCR. EP, experimental periodontitis. ** $P<0.01$, *** $P<0.001$, **** $P<0.0001$

below (volume = length × width^2 × 0.5). On day 25 after the xenograft set-up, all the animals were euthanized. Figure 2A displayed the flowchart for the management plan.

The animal procedures were favored by the ethics committee of Stomatological Hospital of Shandong University (No. 20220907).

Collection of clinical samples

Twelve cases of paraffin-embedded blocks of oral squamous cell carcinoma (OSCC) tissues from Qilu Hospital of Shandong University were collected (OSCC with periodontitis, n = 6; OSCC without periodontitis, n = 6). All patients were first diagnosed with OSCC and had not been given any treatment at the time point of sample collection. Periodontitis was diagnosed based on radiographic alveolar bone loss [14]. In this study, two non-adjacent teeth with bone involved most severely were chosen from all dentition and measurements of alveolar bone loss were made from the cementoenamel junction to the tooth apex (total root length) and from the cementoenamel junction to the marginal bone crest (total bone loss). The proportion of the bone loss of the teeth was calculated according to the formula: (total bone loss-2)/(total root length-2) × 100%. There is no bone loss in non-periodontitis patients, and the distance from the marginal bone crest to the cementoenamel junction is within 2 mm. The data on alveolar bone loss in patients with periodontitis are listed in Supplementary file 2: Table S1. The use of human samples for this study was approved by the ethics committee of scientific research of Shandong University Qilu Hospital (No. KYLL-2017–256).

Micro-Computed Tomography (Micro-CT) analysis

Mouse maxillary alveolar bone was scanned with a liveanimal imaging system (Quantum GX2, PerkinElmer, Japan). In compliance with the software instructions, three-dimensional (3D) images were produced and analyzed.

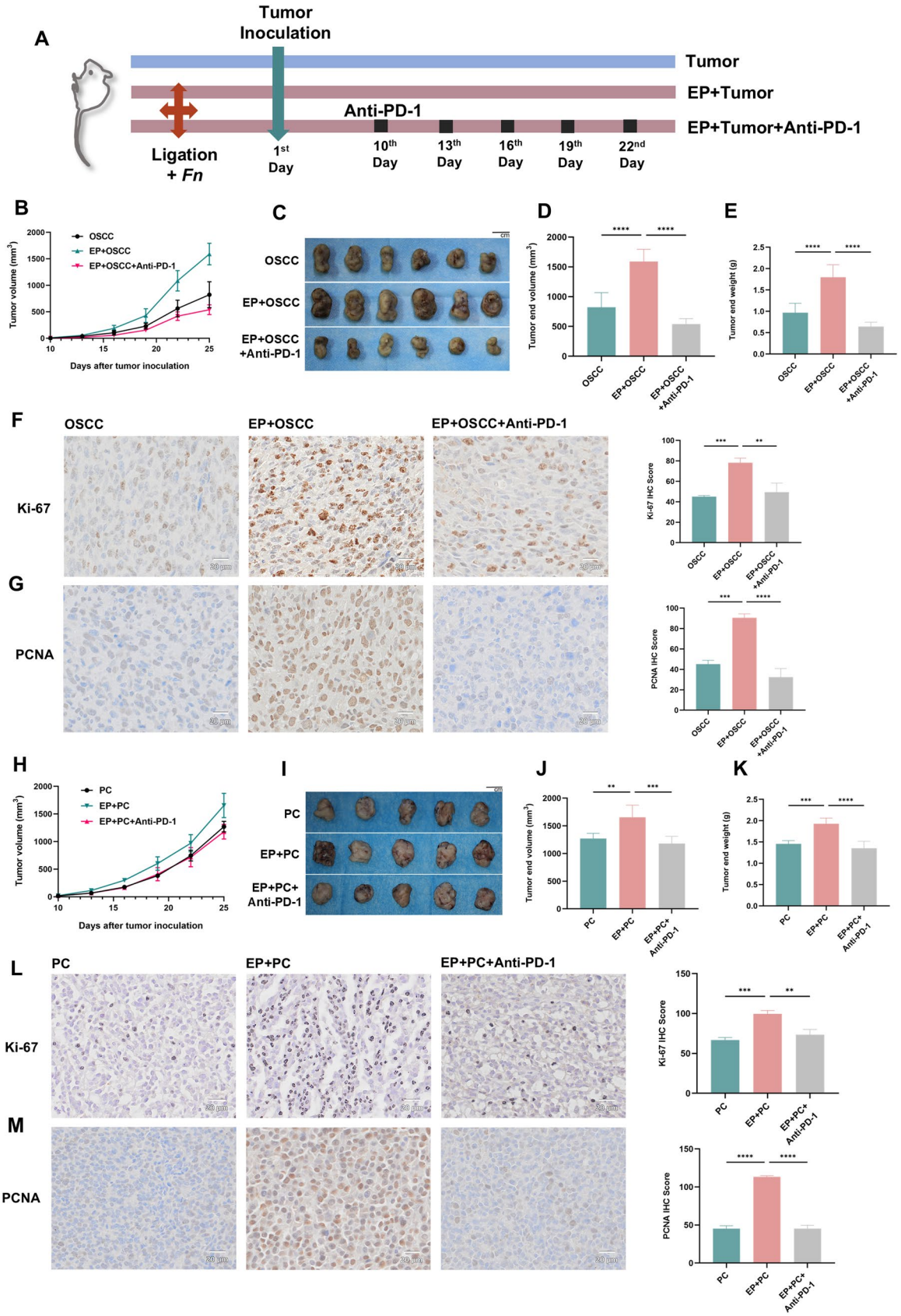
A
Tumor Inoculation
Tumor
EP+Tumor
Anti-PD-1
EP+Tumor+Anti-PD-1
Ligation + Fn
1st Day
10th Day
13th Day
16th Day
19th Day
22nd Day
B
OSCC
EP+OSCC
EP+OSCC+Anti-PD-1
Tumor volume (mm3)
Days after tumor inoculation
C
D
Tumor end volume (mm3)
E
Tumor end weight (g)
F
Ki-67
Ki-67 IHC Score
G
PCNA
PCNA IHC Score
H
PC
EP+PC
EP+PC+Anti-PD-1
I
J
K
L
M

◂**Fig. 2** Periodontitis promotes tumor growth in oral and prostate cancers. **A** Flowchart of animal experiment. **B** SCC7 tumor volumes were recorded during the experiment. **C** Isolated SCC7 tumors from each group of mice. **D, E** Tumor volume (**D**) and tumor weight (**E**) were demonstrated. (n = 6 for each group) **F, G** IHC staining and IHC scores of Ki-67 (**F**) and PCNA (**G**) protein in mouse SCC7 tumor sections. **H** RM-1 tumor volumes were recorded during the experiment. **I** Isolated RM-1 tumors from each group of mice. **J, K** Tumor volume (**J**) and tumor weight (**K**) were demonstrated. (n = 5 for each group) **L, M** IHC staining and IHC scores of Ki-67 (**L**) and PCNA (**M**) protein in mouse RM-1 tumor sections. *Fn*, *Fusobacterium nucleatum*; EP, experimental periodontitis; OSCC, oral squamous cell carcinoma; PC, prostate cancer. ** $P < 0.01$, *** $P < 0.001$, **** $P < 0.0001$

Flow cytometry analysis

The single-cell suspensions from spleen or tumor were stained using Zombie Aqua™ Fixable Viability Kit (Cat. #423101, BioLegend, USA) before blocked with TruStain FcX™ PLUS (anti-mouse CD16/32) Antibody (Cat. #156603, BioLegend, USA) and were then stained for 20–40 min in the dark on ice or at room temperature with the antibodies. The reactions were terminated by PBS. The data were acquired using a CytoFLEX S flow cytometer and analyzed using FlowJo software. All antibodies are listed in Supplementary file 1: Table S1.

Hematoxylin and eosin (HE), immunohistochemistry (IHC) and immunofluorescence (IF) staining

For HE staining, the tumors were fixed in 4% paraformaldehyde and embedded in paraffin wax. The sections were cut at 5 μm thickness. The HE Staining Kit was purchased from Beijing Solarbio Science & Technology Co., Ltd. (Servicebio, China). Then the sections were stained according to the manufacturer's guidelines. For IHC staining, the sections were treated with a Tris–EDTA antigen retrieval solution (Beyotime, China) and incubated with primary antibodies. And a universal 2-step test kit (ZSGB-BIO, China) was used for the next steps. For IF staining, the sections were then blocked in 10% goat serum albumin (ZSGB-BIO, China) and incubated with primary antibodies at 4 °C overnight. Next, secondary antibodies and 4',6-diamidino-2-phenylindole (DAPI) (Servicebio, China) were incubated successively. All antibodies are listed in Supplementary file 1: Table S2.

RNA extraction and quantitative real-time Polymerase Chain Reaction (qRT-PCR)

Total RNA was extracted by the TRIzol reagent (Invitrogen, USA) and was subsequently transformed in reverse into cDNA with the Hifair® III 1st Strand cDNA Synthesis SuperMix (Yeasen, China). qRT-PCR was conducted with SYBR Premix Ex Taq (Yeasen, China) on a Light Cycler II Real-time PCR system (Roche, Switzerland). The $2^{-\Delta\Delta Ct}$ method was utilized and target gene expression was standardized to glyceraldehyde-3-phosphate dehydrogenase (GAPDH). Primers utilized are provided in Supplementary file 1: Table S3.

Culture of THP-1-derived macrophages in Cal-27 cell conditioned media (CM)

Cal-27 cells were separated into two groups: (1) Control group: the cells were cultivated in complete DMEM media, (2) LPS-stimulated group: the cells were cultivated in complete DMEM media with 10 μg/ml *Pg*-LPS (InvivoGen, USA). After 24 h, two groups of cells were cleaned three times using serum-free media and subsequently cultured for an additional 24 h in serum-free media to collect the CM. Next, THP-1 cells were activated by phorbol 12-myristate 13-acetate (PMA, 100 ng/ml) and grown separately in the CM. Figure 7A presented the flowchart of the experiment.

Western blotting (WB)

Total protein from THP-1 cells was extracted with radioimmunoprecipitation assay lysis buffer containing protease inhibitor (Beyotime, China). Primary antibodies against PD-L1 (1:7000, Proteintech, USA) and GAPDH (1:10,000, Proteintech, USA) were used. WB was executed as described [15]. ImageJ software was used to analyze and GAPDH was employed as a control.

Cell IF staining

After being fixed for 30 min with 4% paraformaldehyde, THP-1 cells were blocked for 1 h with 10% goat serum. After that, cells were treated with primary antibody against PD-L1 (1:200, Proteintech, USA) overnight at 4 °C, then CoraLite® Plus 488 conjugated goat anti-mouse secondary antibody (1:200, Proteintech, USA) and DAPI (Servicebio, China) were incubated successively.

Fluorescence in situ hybridization (FISH)

FISH was used to detect *Fn* in paraffin-embedded tissue sections. We bought the *Fn*-targeted probe (5′-CGCAAT ACAGAGTTGAGCCCTGC-3′) and FISH kit from Guangzhou EXON Biological Technology company (Guangzhou, China). Then the sections were deparaffinized, rehydrated and hybridized by the probe according to the manufacturer's guidelines.

Statistical analysis

The statistical analysis was performed using GraphPad Prism 9.5 software (GraphPad Software) and data are presented as the mean ± standard deviation (SD) for three independent experiments at least. A one-way ANOVA was employed for comparisons among multiple groups and two-tailed unpaired Student's t test was utilized for comparisons between two groups. $P < 0.05$ was regarded as significant statistically.

Results

Modeling of an experimental periodontitis

We constructed an experimental mouse periodontitis model with silk ligation and *Fn* infection to investigate the effect of periodontitis on tumor progression (Fig. 1A). In the experimental periodontitis group, HE staining showed loss of connective tissue attachment as well as severe alveolar bone resorption compared to the control group (Fig. 1B). 3D reconstructed images also revealed a significant reduction of alveolar bone height in the group with experimental periodontitis (Fig. 1C). Gingival tissues were obtained from ligation sites for qRT-PCR analysis and the experimental periodontitis group showed significantly elevated levels of inflammatory factors IL-6, IL-1β and tumor necrosis factor-α (TNF-α) compared with the control (Fig. 1D). These findings indicated that an experimental mouse periodontitis model was successfully established.

Periodontitis promotes tumor growth in oral and prostate cancers

Recently, Shi et al. reported that experimental periodontitis facilitated colorectal cancer advancement and immunosuppressive microenvironment [11], yet it remains largely unclear whether periodontitis can also exert similar effect on other tumors. Thus, a mouse periodontitis model was pre-established prior to subcutaneous establishment of a xenograft tumor model and with or without subsequent anti-PD-1 treatment (Fig. 2A). Periodontitis promoted tumor progression in oral (Fig. 2B-E) and prostate (Fig. 2H-K) cancer models, as evaluated by tumor volume and weight, compared with the control group. Meanwhile, IHC results also demonstrated that mice in the periodontitis group expressed more cell proliferation markers Ki-67 and PCNA (Fig. 2F, G and L, M). Collectively, these results suggest that periodontitis facilitates the progression of oral and prostate cancers. However, the experimental results conducted by FISH on paraffin-embedded tissue sections showed that *Fn* was not found in oral cancer tissues and prostate cancer tissues (Supplementary file 2: Fig. S1), suggesting that chronic low-grade inflammation may play a more important pro-cancer role than direct effect of *Fn*.

Periodontitis contributes to iTME

In the tumor microenvironment (TME), immune-suppressive cells, including Tregs and TAMs, suppress the activity of $CD8^+$T cells and play a major part in tumor pathogenesis [16]. To observe whether periodontitis enhances iTME, a variety of immune cells were examined of the control and periodontitis groups in the context of oral and prostate cancers. In oral cancer tumor model, tumor-infiltrating and extratumoral lymphocytes were assayed by flow cytometry and IF. The proportions of $CD8^+$T cells in spleen (Fig. 3A) and tumor (Fig. 3B), and the percentage of IFN-γ^+CD8^+T cells in tumor (Fig. 3G) of the periodontitis group were lower than those of the control group, while the ratios of Tregs in spleen (Fig. 3C) and tumor (Fig. 3D), and M2-TAMs in spleen (Fig. 3E) and tumor (Fig. 3F) of the group with periodontitis were significantly higher than the without. Moreover, IF assay for clinical OSCC samples also revealed that the proportions of IFN-γ^+CD8^+T cells of the group with periodontitis declined (Fig. 3H). In prostate cancer model, similar results were found in the decreased ratios of $CD8^+$T cells in spleen (Fig. 4A) and tumor (Fig. 4B), and the ratio of IFN-γ^+CD8^+T cells in tumor (Fig. 4F), as well as the increased percentage of Tregs in spleen (Fig. 4C), and M2-TAMs in spleen (Fig. 4D) and tumor (Fig. 4E) of the group with periodontitis compared to the without. The above outcomes demonstrate that periodontitis enhances iTME, which is in line with the findings of Shi et al. [11].

Periodontitis enhances suppressive immune checkpoint molecule PD-1/PD-L1 expression

Interaction of PD-L1 and PD-1 makes a great contribution to iTME [17]. To explore whether periodontitis-enhanced immunosuppression is related to PD-1/PD-L1, the expression profiles of PD-1/PD-L1 were examined in the TME. Flow cytometry demonstrated that in oral cancer model, the proportions of PD-1^+CD8^+T cells in tumor (Fig. 5A), and PD-$L1^+$TAMs in spleen (Fig. 5B) and tumor (Fig. 5C) significantly increased in the periodontitis group compared to the control group. IF staining also showed that the ratios of PD-1^+CD8^+T cells (Fig. 5E) and PD-$L1^+$TAMs (Fig. 5F) in the periodontitis group significantly elevated, further evidenced in clinical OSCC samples (Fig. 5G, H). IHC staining showed that PD-L1 expression level in the group with periodontitis was significantly higher than the without (Fig. 5D). In prostate cancer, there was also a significant rise in PD-L1 expression (Fig. 6A) and the percentage of PD-1^+CD8^+T cells (Fig. 6B) of the tumor in the periodontitis

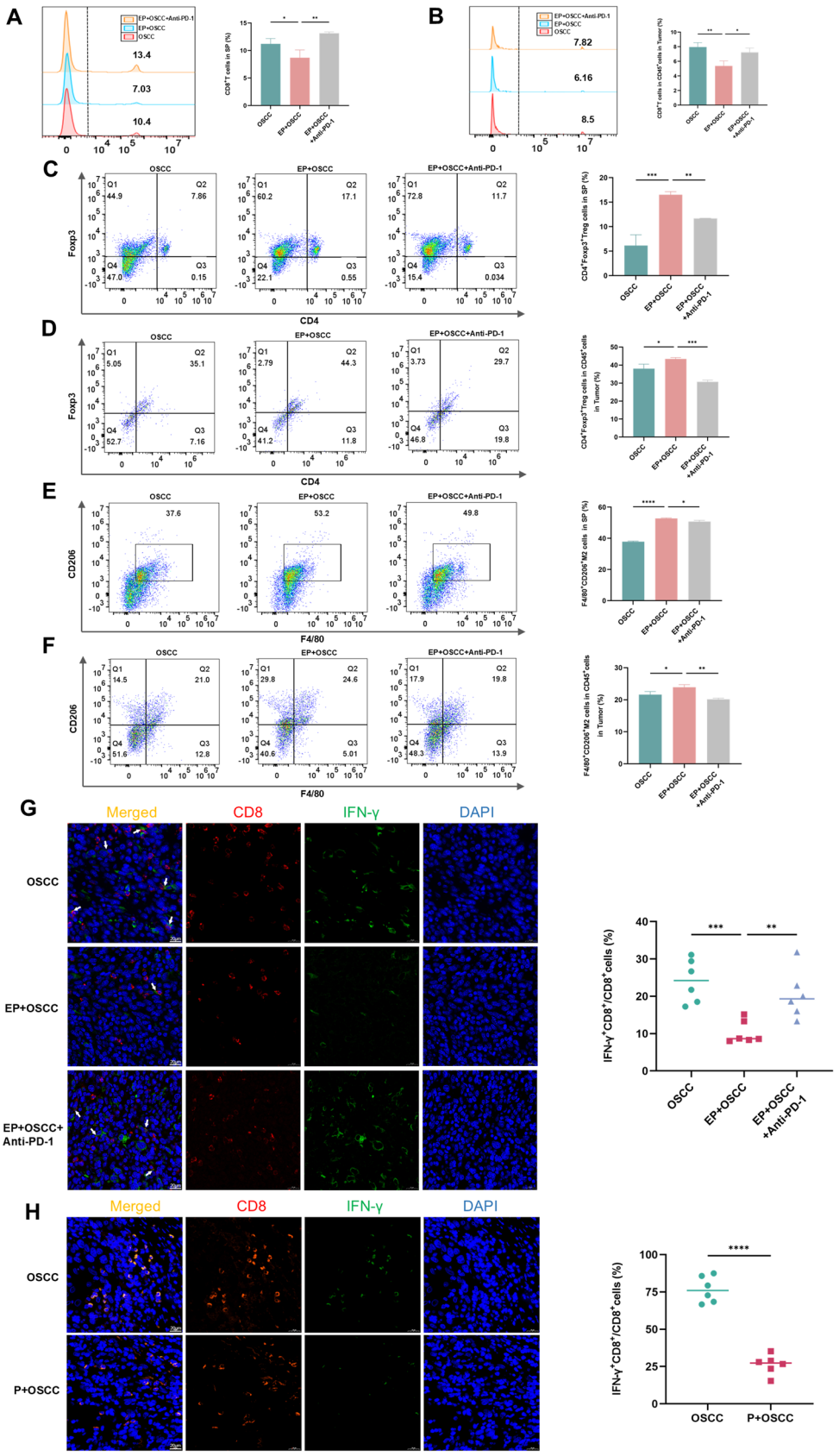

Fig. 3 Periodontitis contributes to iTME in oral cancer. **A-F** Flow cytometry images and quantitative levels of $CD8^+$T cells in spleen (**A**) and tumor (**B**), $CD4^+Foxp3^+$Treg cells in spleen (**C**) and tumor (**D**), $F4/80^+CD206^+$M2 cells in spleen (**E**) and tumor (**F**) from each group. **G, H** IF staining and quantitative levels of IFN-γ^+CD8^+T cells in SCC7 (**G**) and clinical OSCC (**H**) tumor sections from each group. SP, spleen; P, periodontitis; EP, experimental periodontitis; OSCC, oral squamous cell carcinoma. * $P<0.05$, ** $P<0.01$, *** $P<0.001$, **** $P<0.0001$

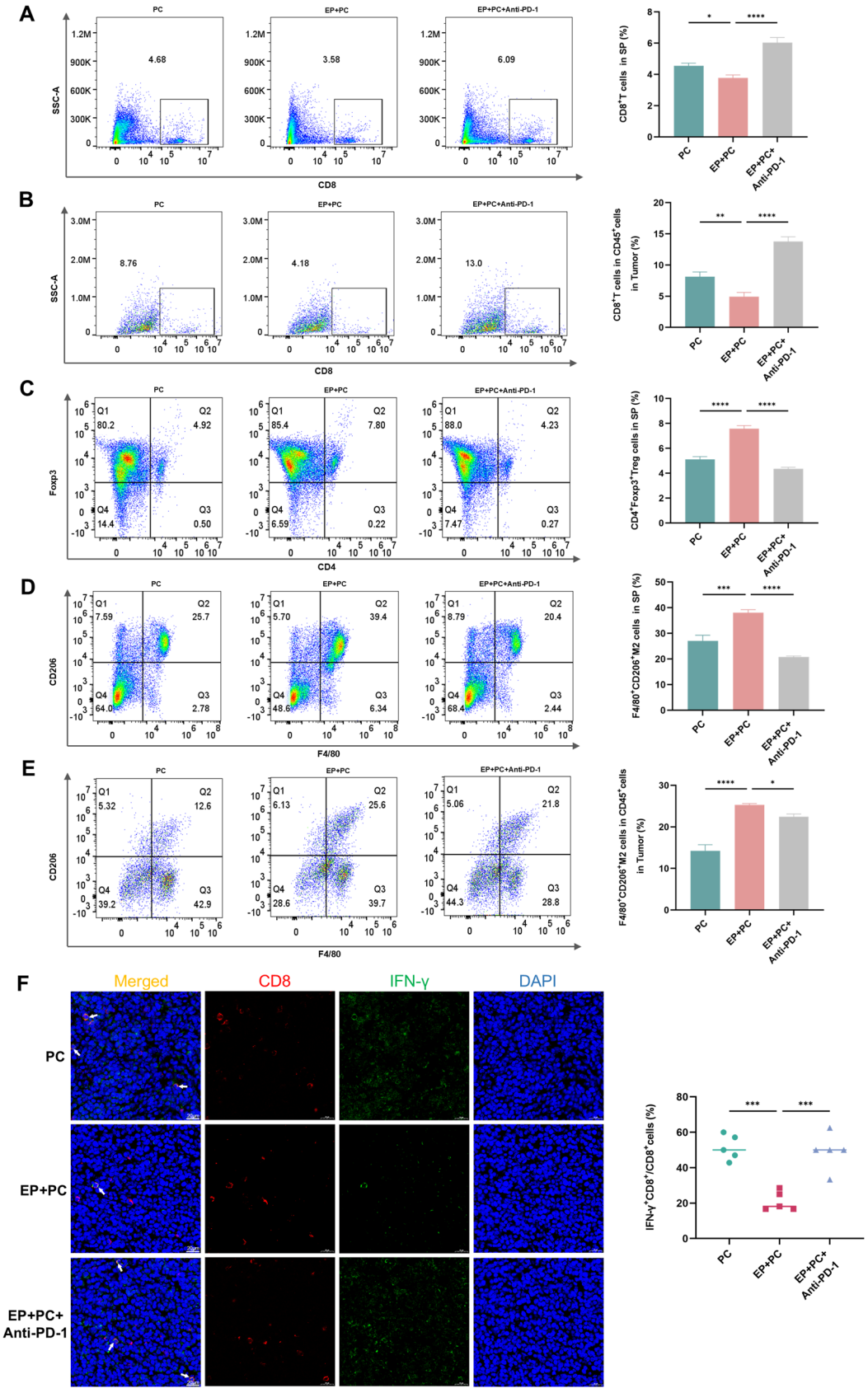
A
PC
EP+PC
EP+PC+Anti-PD-1
SSC-A
CD8
4.68
3.58
6.09
CD8+T cells in SP (%)
B
8.76
4.18
13.0
CD8+T cells in CD45+cells in Tumor (%)
C
Foxp3
CD4
Q1 80.2
Q2 4.92
Q3 0.50
Q4 14.4
Q1 85.4
Q2 7.80
Q3 0.22
Q4 6.59
Q1 88.0
Q2 4.23
Q3 0.27
Q4 7.47
CD4+Foxp3+Treg cells in SP (%)
D
CD206
F4/80
Q1 7.59
Q2 25.7
Q3 2.78
Q4 64.0
Q1 5.70
Q2 39.4
Q3 6.34
Q4 48.6
Q1 8.79
Q2 20.4
Q3 2.44
Q4 68.4
F4/80+CD206+M2 cells in SP (%)
E
Q1 5.32
Q2 12.6
Q3 42.9
Q4 39.2
Q1 6.13
Q2 25.6
Q3 39.7
Q4 28.6
Q1 5.06
Q2 21.8
Q3 28.8
Q4 44.3
F4/80+CD206+M2 cells in CD45+cells in Tumor (%)
F
Merged
CD8
IFN-γ
DAPI
PC
EP+PC
EP+PC+ Anti-PD-1
IFN-γ+CD8+/CD8+cells (%)

◂**Fig. 4** Periodontitis contributes to iTME in prostate cancer. **A-E** Flow cytometry images and quantitative levels of $CD8^+$T cells in spleen (**A**) and tumor (**B**), $CD4^+Foxp3^+$Treg cells in spleen (**C**), $F4/80^+CD206^+$M2 cells in spleen (**D**) and tumor (**E**) from each group. **F** IF staining and quantitative level of IFN-γ^+CD8^+T cells in tumor sections from each group. SP, spleen; EP, experimental periodontitis; PC, prostate cancer. * $P<0.05$, ** $P<0.01$, *** $P<0.001$, **** $P<0.0001$

group compared with the control. The findings presented above suggest that periodontitis encourages PD-1/PD-L1 expression in the TME.

LPS boosts PD-L1 expression in macrophages under TME

The above results have demonstrated that periodontitis increased macrophages expressing PD-L1 molecule in the TME, so we next examined whether this phenomenon also existed in vitro. To probe this, we stimulated Cal-27 cells with PBS or 10 μg/ml LPS and then collected CM separately. The CM were then used to stimulate macrophages and observe PD-L1 molecule expression (Fig. 7A). In agreement with the results of in vivo experiments, the LPS-stimulated group showed elevated PD-L1 gene level (Fig. 7B). Apart from that, both WB and IF results also demonstrated increased PD-L1 protein level in the LPS-stimulated group (Fig. 7C, D). Altogether, these findings show that inflammation stimulation could boost PD-L1 expression in macrophages under TME.

PD-1/PD-L1 blockage reduces the pro-cancer efficacy of periodontitis

All the above findings reveal that periodontitis promotes tumor progression, immune evasion and PD-1/PD-L1 expression. In order to further explore whether PD-1/PD-L1 mediates the promotive effect of periodontitis on tumor progression and immune escape, the anti-PD-1 test was performed on the periodontitis mice after the specialty of RMP1-14, anti-mouse PD-1 antibody had been demonstrated (Supplementary file 2: Fig. S2 and Fig. S3). After anti-PD-1 therapy, the tumor volume and weight significantly reduced (Fig. 2B-E in OSCC and H–K in PC) and the expression of Ki-67 and PCNA also decreased (Fig. 2F, G in OSCC and L, M in PC) compared with the periodontitis group. Additionally, the levels of IFN-γ^+CD8^+T cells and $CD8^+$T cells elevated in the anti-PD-1 group (Fig. 3A, B, G in OSCC and Fig. 4A, B, F in PC), while the proportions of Tregs and M2-TAMs markedly declined (Fig. 3C-F in OSCC and Fig. 4C-E in PC) after treatment with anti-PD-1. All in all, these results point out that PD-1/PD-L1 blockade with anti-PD-1 treatment effectively suppresses the tumor-promoting effect of periodontitis. And this further validates that the pro-cancer, increased immunosuppressive microenvironmental effect of periodontitis might be induced by augmenting PD-1/PD-L1 (Fig. 8).

Discussion

Chronic inflammation can create an environment that is conducive to the initiation and advancement of cancer and has been indicated to be related to several cancer types, such as prostate, lung, colorectal, liver and breast cancers [18, 19]. Periodontitis, a chronic inflammation initiated by microbial infection, is also closely related to the development of cancer. However, most research has been limited to investigating the relationship of periodontal pathogenic bacteria, including *Pg* and *Fn*, in the advancement of cancer [8, 9]. The inflammatory response caused by periodontal pathogenic bacterial infection does not fully represent the systemic inflammatory state induced by periodontitis. Therefore, we established an experimental periodontitis model by silk ligation plus *Fn* infection to better explore the mechanisms of periodontitis in cancer. Our results show that periodontitis promotes the growth of oral and prostate cancers and iTME formation, consistent with the findings of Shi et al. [11]. Furthermore, we novelly reveal that the enhanced immune checkpoint molecule expression is associated with the pro-cancer activity of periodontitis.

In the TME, TAMs, Tregs and MDSCs serve as immunosuppressive cells to suppress $CD8^+$T cell activity and play an indispensable part in tumor pathogenesis [16]. LPS-mediated chronic inflammation induced iTME characterized by the accumulation of MDSCs and Tregs, resulting in T-cell exhaustion and enhancing NNK-induced lung tumorigenesis [20]. *Pg* and *Fn*, two important pathogenic bacteria in periodontitis, facilitated tumorigenesis by generating a cancer-promoting microenvironment [9, 21]. Moreover, obesity characterized by chronic low-grade inflammation similar to periodontitis is strongly associated with iTME [22, 23]. Nevertheless, whether periodontitis as a disease entity enhances iTME has been rarely studied. Shi et al. recently reported that experimental periodontitis promoted the progression of colitis-associated colorectal cancer and led to the increase in Th2 cells, Tregs and PD-1^+CD8^+T cells in spleen [11]. Our present research suggested that the periodontitis group not only exhibited a higher presence of immune-suppressive cells, including TAMs, Tregs and PD-1^+CD8^+T cells, but demonstrated a lower level of IFN-γ^+CD8^+T cells and $CD8^+$T cells than the control group. Given that TAMs and Tregs possess inhibition on cytotoxic T cells [24], and PD-1^+CD8^+T cells as well as IFN-γ^+CD8^+T cells are separately the exhausted and the activated status of T cells [25, 26], our results imply that periodontitis promotes tumor immune escape in oral and prostate cancers, which coincides with the

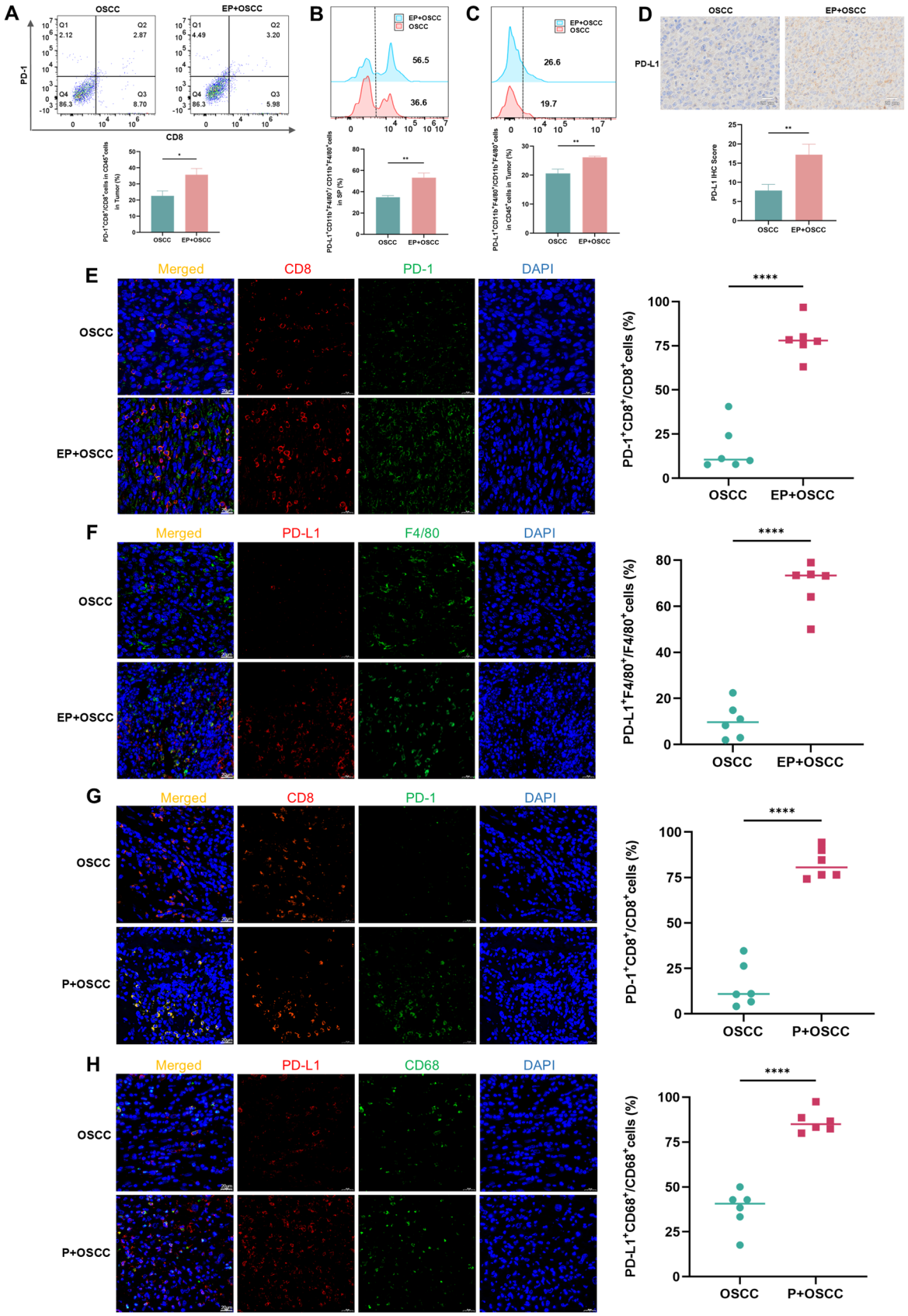
A
OSCC
EP+OSCC
PD-1
CD8
Q1
Q2
Q3
Q4
2.12
2.87
86.3
8.70
4.49
3.20
86.3
5.98
B
EP+OSCC
OSCC
56.5
36.6
C
EP+OSCC
OSCC
26.6
19.7
D
OSCC
EP+OSCC
PD-L1
PD-L1 IHC Score
E
Merged
CD8
PD-1
DAPI
OSCC
EP+OSCC
PD-1+CD8+/CD8+cells (%)
F
Merged
PD-L1
F4/80
DAPI
OSCC
EP+OSCC
PD-L1+F4/80+/F4/80+cells (%)
G
Merged
CD8
PD-1
DAPI
OSCC
P+OSCC
PD-1+CD8+/CD8+cells (%)
H
Merged
PD-L1
CD68
DAPI
OSCC
P+OSCC
PD-L1+CD68+/CD68+cells (%)

◂**Fig. 5** Periodontitis enhances PD-1/PD-L1 expression in oral cancer. **A-C** Flow cytometry images and quantitative levels of PD-1$^+$CD8$^+$cells in tumor (**A**), PD-L1$^+$CD11b$^+$F4/80$^+$cells in spleen (**B**) and tumor (**C**) from each group. **D** IHC staining and IHC scores of PD-L1 protein in SCC7 tumor sections from each group. **E, F** IF staining and quantitative levels of PD-1$^+$CD8$^+$cells (**E**) and PD-L1$^+$F4/80$^+$cells (**F**) in SCC7 tumor sections from each group. **G, H** IF staining and quantitative levels of PD-1$^+$CD8$^+$cells (**G**) and PD-L1$^+$CD68$^+$cells (**H**) in clinical OSCC tumor sections from each group. SP, spleen; P, periodontitis; EP, experimental periodontitis; OSCC, oral squamous cell carcinoma. ** $P<0.01$, *** $P<0.001$, **** $P<0.0001$

results of Shi et al. on colitis-associated colorectal cancer [11].

It is widely known that PD-L1 and PD-1 are crucial immunosuppressive molecules in the TME, which are intimately associated with the anti-cancer immunity of the organism [27]. PD-1 could be upregulated on activated T cells, resulting in immune tolerance [28]. Tumor cells [29] and TAMs [30] frequently overexpress the ligand for PD-1, PD-L1, to facilitate escaping from the immune system. PD-L1 inhibits T-cell activation and effector functions, thereby impacting their ability to regulate tumors. Anti-PD-L1 therapy raises T-cell infiltration and IFN-γ generation, and inhibits tumor development in mouse models [31]. Additionally, PD-1/PD-L1 conjugation not merely results in T-cell suppression but contributes to an immune-suppressive macrophage phenotype [17]. A growing body of research indicates that PD-1/PD-L1 expression in the TME is influenced by chronic inflammation or infection [20, 32] as well as by periodontal pathogenic bacteria [8, 33]. PD-1 and PD-L1 are also increased in peripheral blood and periodontal tissue among patients with periodontitis [34, 35]. Here, we innovatively discovered that periodontitis assisted the growth of tumors by influencing local and systemic PD-1/PD-L1 expression in oral and prostate cancers. Anti-PD-1 treatment attenuated the cancer-encouraging effect of periodontitis, indicating that PD-1/PD-L1 could be a mechanistic link between periodontitis and tumor immunosuppression.

PD-L1 is expressed in various cells, including TAMs, which constitute the majority of PD-L1-expressing cells [36]. TAMs express PD-L1 and contribute to iTME. Macrophages could capture the administrated anti-PD-1 antibody from the T cell surface within minutes and affect the outcomes of anti-PD-1 treatment depending on their Fcγ-receptors (FcγRs) [37], implying that FcγRs on macrophages are also immunosuppressive factors. We found that the proportion of TAMs-expressing FcγRs (FcγRIIb/III) was elevated in periodontitis group (Supplementary file 2: Fig. S4). This suggests that periodontitis not merely encourages tumor

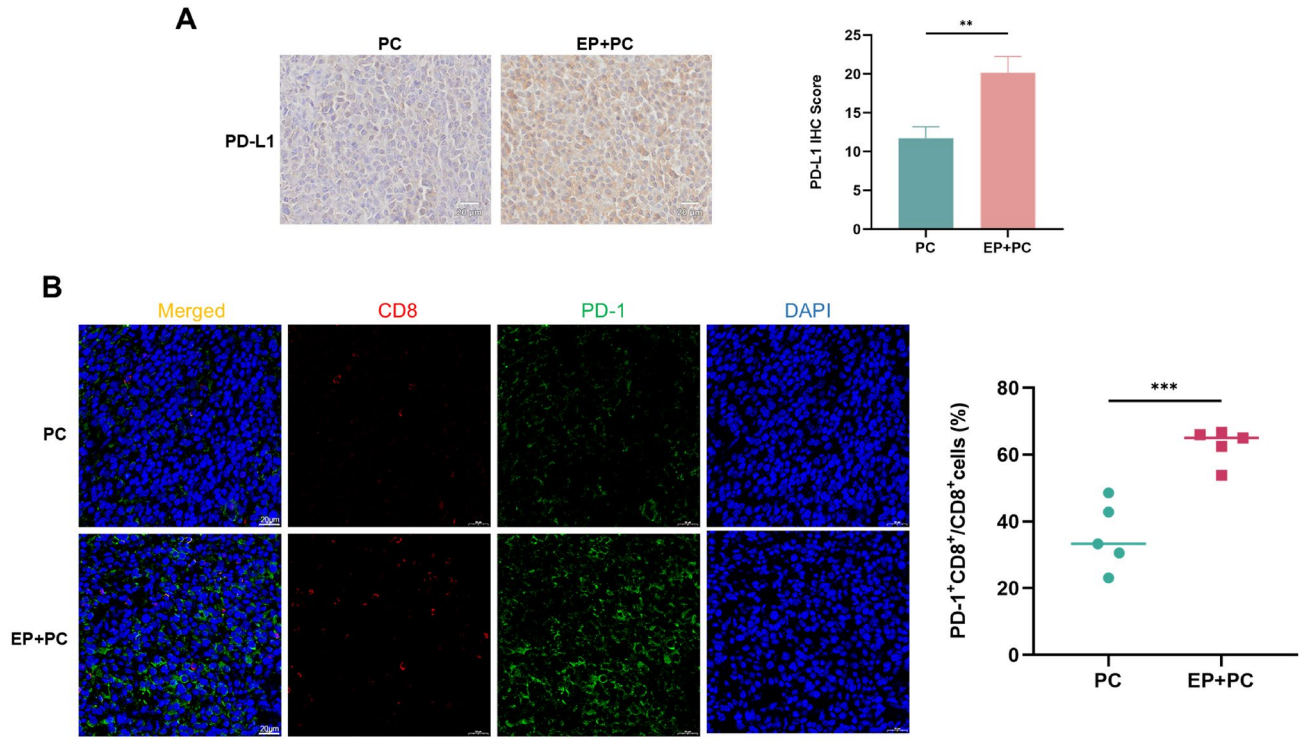

Fig. 6 Periodontitis enhances PD-1/PD-L1 expression in RM-1 xenograft. **A** IHC staining and IHC scores of PD-L1 protein in RM-1 tumor sections from each group. **B** IF staining and quantitative level of PD-1$^+$CD8$^+$cells in RM-1 tumor sections from each group. EP, experimental periodontitis; PC, prostate cancer. ** $P<0.01$, *** $P<0.001$

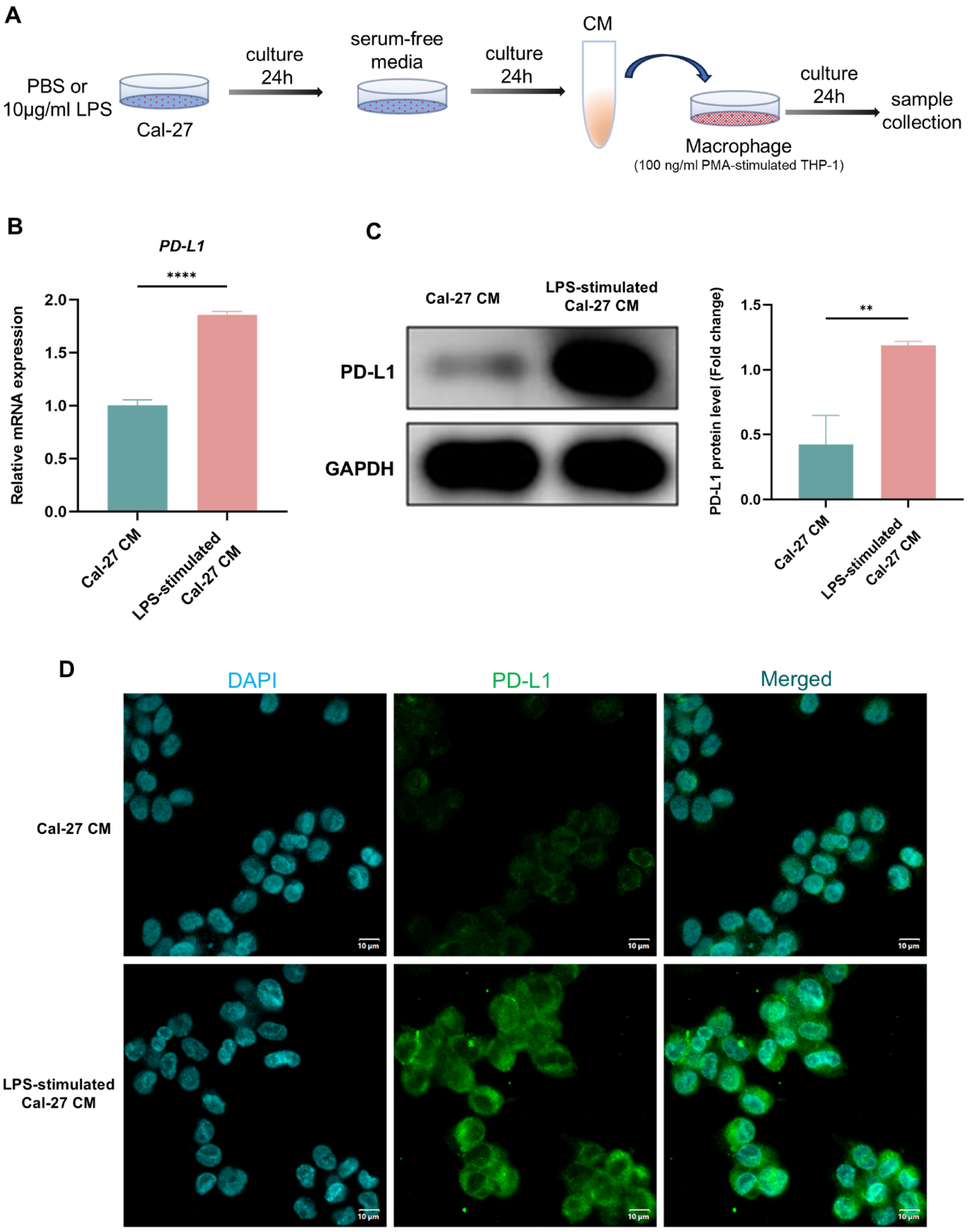

Fig. 7 LPS boosts PD-L1 expression in macrophages under TME. **A** Flowchart of cell experiment. **B** PD-L1mRNA level of THP-1-derived macrophages in each group measured by qRT-PCR. **C** WB showing the expression and quantitative level of PD-L1 protein in each group. **D** IF staining of PD-L1 in each group. CM, conditioned media. ** $P < 0.01$, **** $P < 0.0001$

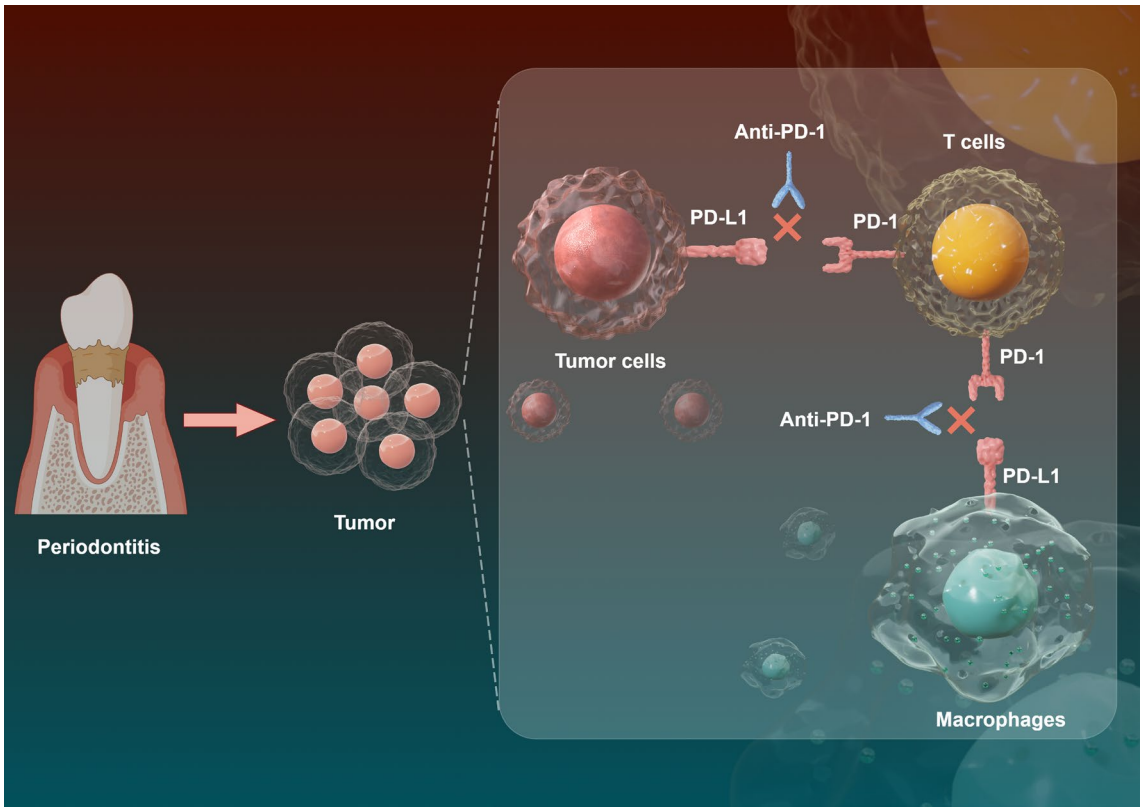

Fig. 8 The schematic diagram of periodontitis promoting tumor progression. Periodontitis promotes tumor development and anti-PD-1 therapy attenuates the cancer-promoting effect of periodontitis

development, but perhaps also exerts an affection on tumor immunotherapy.

The mechanism by which periodontitis is involved in the increase of Treg cells remains largely unclear, but there are multiple possibilities. Francisco et al. have reported that PD-L1-coated beads can induce Tregs in vitro, PD-L1 increases Foxp3 expression and enhances the immunosuppressive ability of Tregs. Moreover, PD-L1 could convert naive $CD4^{+}$T cells to Tregs through the downregulation of Akt, mTOR and ERK2 and the simultaneous upregulation of PTEN [38]. The intratumoral IL-1 receptor type 1 (IL1R1) $^{+}$ Treg cells are clonally expanded with stronger suppressive function compared to $IL1R1^{-}$ Treg cells [1]. Thus, the increased levels of PD-L1 and IL-1 may be partial factors for periodontitis-enhanced increase of Treg cells in TME.

Conclusions

In summary, we innovatively demonstrate that periodontitis may contribute to tumor progression and immune escape by encouraging PD-1/PD-L1 expression, providing new insight into the underlying mechanism by which periodontitis affects tumor tumorigenesis and development. However, more questions associated with the potential effect of periodontitis on tumor immunosuppression and immunotherapy require further investigation. Firstly, both periodontal pathogenic bacteria [39] and aseptic chronic inflammation such as obesity [40] can contribute to tumor progression, whereas periodontitis may result in bacteremia as well as systemic chronic inflammation, thus, which of the two factors plays a greater role in the cancer-promoting effect of periodontitis is not yet clear. Secondly, some studies show that PD-L1 is a predictor of tumor immunotherapy efficacy [41], yet others demonstrate that PD-L1 increases immunotherapy resistance [42]. Exact function of periodontitis-elevated PD-L1 in tumor immunotherapy needs to be further explored. Thirdly, standard mechanical treatment of periodontitis can control periodontal inflammation. However, the effect of local treatment of periodontal disease on tumor immunosuppression and immunotherapy response requires to be enlightened.

Supplementary Information The online version contains supplementary material available at https://doi.org/10.1007/s00262-024-03865-5.

Acknowledgements We are very thankful to Figdraw (www.figdraw.com) for the picture material.

Author contributions SW and PY conceived and designed the research. SW, FN, QY, HT, PG, JJ, and JL carried out the experiments and analyzed the data. SW, FN, PY, and CY wrote, reviewed, and edited the manuscript. PY and CY supervised the research and provided funding support. All authors reviewed and approved the final manuscript.

Funding This work was supported by the Province Natural Science Foundation of Shandong Province (No. ZR2022MH136), Key R&D Program of Shandong Province, China (No. 2021SFGC0502), Construction Engineering Special Fund of "Taishan Scholars" of Shandong Province (No. ts20190975) and National Natural Science Youth Foundation of China (No. 81702684).

Data availability All data presented in the current study are available from the corresponding author on reasonable request.

Declarations

Conflict of interest The authors declare that they have no conflict of interest.

Ethics approval All animal research was performed in accordance with the Basel Declaration and approved by the ethics committee of Stomatological Hospital of Shandong University (No. 20220907). The use of human samples for this study was performed in accordance with the Declaration of Helsinki and approved by the ethics committee of scientific research of Shandong University Qilu Hospital (No. KYLL-2017–256).

References

1. Mair F, Erickson JR, Frutoso M et al (2022) Extricating human tumour immune alterations from tissue inflammation. Nature 605:728–735. https://doi.org/10.1038/s41586-022-04718-w
2. Beatty GL, Gladney WL (2015) Immune escape mechanisms as a guide for cancer immunotherapy. Clin Cancer Res 21:687–692. https://doi.org/10.1158/1078-0432.Ccr-14-1860
3. Yaguchi T, Kawakami Y (2016) Cancer-induced heterogeneous immunosuppressive tumor microenvironments and their personalized modulation. Int Immunol 28:393–399. https://doi.org/10.1093/intimm/dxw030
4. Mantovani A, Allavena P, Sica A, Balkwill F (2008) Cancer-related inflammation. Nature 454:436–444. https://doi.org/10.1038/nature07205
5. Hajishengallis G (2015) Periodontitis: from microbial immune subversion to systemic inflammation. Nat Rev Immunol 15:30–44. https://doi.org/10.1038/nri3785
6. Nwizu N, Wactawski-Wende J (2000) Genco RJ (2020) Periodontal disease and cancer: Epidemiologic studies and possible mechanisms. Periodontol 83:213–233. https://doi.org/10.1111/prd.12329
7. Chen SH, Chen JF, Hung YT, Hsu TJ, Chiu CC, Kuo SJ (2023) Exploring the relationship between periodontitis anti-periodontitis, therapy, and extra-oral cancer risk: findings from a nationwide population-based study. Biomedicines. https://doi.org/10.3390/biomedicines11071949
8. Ren J, Han X, Lohner H, Hoyle RG, Li J, Liang S, Wang H (2023) P. Gingivalis infection upregulates PD-L1 expression on dendritic cells, suppresses CD8+ T cell responses, and aggravates oral cancer. Cancer Immunol Res. https://doi.org/10.1158/2326-6066.Cir-22-0541
9. Kostic AD, Chun E, Robertson L et al (2013) Fusobacterium nucleatum potentiates intestinal tumorigenesis and modulates the tumor-immune microenvironment. Cell Host Microbe 14:207–215. https://doi.org/10.1016/j.chom.2013.07.007
10. Groeger S, Wu F, Wagenlehner F, Dansranjav T, Ruf S, Denter F, Meyle J (2022) PD-L1 Up-Regulation in prostate cancer cells by porphyromonas gingivalis. Front Cell Infect Microbiol 12:935806. https://doi.org/10.3389/fcimb.2022.935806
11. Shi YT, He JM, Tong ZA et al (2023) Ligature-induced periodontitis drives colorectal cancer: an experimental model in mice. J Dent Res 102:689–698. https://doi.org/10.1177/00220345231158269
12. Pai SI, Matheus HR, Guastaldi FPS (2023) Effects of periodontitis on cancer outcomes in the era of immunotherapy. Lancet Healthy Longev 4:e166–e175. https://doi.org/10.1016/s2666-7568(23)00021-1
13. Abe T, Hajishengallis G (2013) Optimization of the ligature-induced periodontitis model in mice. J Immunol Methods 394:49–54. https://doi.org/10.1016/j.jim.2013.05.002
14. Papapanou PN, Sanz M, Buduneli N et al (2018) Periodontitis: consensus report of workgroup 2 of the 2017 world workshop on the classification of periodontal and peri-implant diseases and conditions. J Clin Periodontol 45(Suppl 20):S162–S170. https://doi.org/10.1111/jcpe.12946
15. Li Y, Xing S, Chen F, Li Q, Dou S, Huang Y, An J, Liu W, Zhang G (2023) Intracellular fusobacterium nucleatum infection attenuates antitumor immunity in esophageal squamous cell carcinoma. Nat Commun 14:5788. https://doi.org/10.1038/s41467-023-40987-3
16. Dongre A, Weinberg RA (2021) Leveraging immunochemotherapy for treating pancreatic cancer. Cell Res 31:1228–1229. https://doi.org/10.1038/s41422-021-00574-x
17. Hartley GP, Chow L, Ammons DT, Wheat WH, Dow SW (2018) Programmed cell death ligand 1 (PD-L1) signaling regulates macrophage proliferation and activation. Cancer Immunol Res 6:1260–1273. https://doi.org/10.1158/2326-6066.Cir-17-0537
18. Taniguchi K, Karin M (2018) NF-κB, inflammation, immunity and cancer: coming of age. Nat Rev Immunol 18:309–324. https://doi.org/10.1038/nri.2017.142
19. Furman D, Campisi J, Verdin E et al (2019) Chronic inflammation in the etiology of disease across the life span. Nat Med 25:1822–1832. https://doi.org/10.1038/s41591-019-0675-0
20. Liu CH, Chen Z, Chen K et al (2021) Lipopolysaccharide-mediated chronic inflammation promotes tobacco carcinogen-induced lung cancer and determines the efficacy of immunotherapy. Cancer Res 81:144–157. https://doi.org/10.1158/0008-5472.Can-20-1994
21. Wen L, Mu W, Lu H et al (2020) Porphyromonas gingivalis promotes oral squamous cell carcinoma progression in an immune microenvironment. J Dent Res 99:666–675. https://doi.org/10.1177/0022034520909312
22. Wang Z, Aguilar EG, Luna JI et al (2019) Paradoxical effects of obesity on T cell function during tumor progression and PD-1

checkpoint blockade. Nat Med 25:141–151. https://doi.org/10.1038/s41591-018-0221-5
23. Ringel AE, Drijvers JM, Baker GJ et al (2020) Obesity shapes metabolism in the tumor microenvironment to suppress anti-tumor immunity. Cell 183:1848–66.e26. https://doi.org/10.1016/j.cell.2020.11.009
24. Cervantes-Villagrana RD, Albores-García D, Cervantes-Villagrana AR, García-Acevez SJ (2020) Tumor-induced neurogenesis and immune evasion as targets of innovative anti-cancer therapies. Signal Transduct Target Ther 5:99. https://doi.org/10.1038/s41392-020-0205-z
25. Siddiqui I, Schaeuble K, Chennupati V et al (2019) Intratumoral Tcf1(+)PD-1(+)CD8(+) T cells with stem-like properties promote tumor control in response to vaccination and checkpoint Blockade immunotherapy. Immunity 50:195-211.e10. https://doi.org/10.1016/j.immuni.2018.12.021
26. St Paul M, Ohashi PS (2020) The Roles of CD8(+) T cell subsets in antitumor Immunity. Trends Cell Biol 30:695–704. https://doi.org/10.1016/j.tcb.2020.06.003
27. Majidpoor J, Mortezaee K (2021) The efficacy of PD-1/PD-L1 blockade in cold cancers and future perspectives. Clin Immunol 226:108707. https://doi.org/10.1016/j.clim.2021.108707
28. Nishimura H, Nose M, Hiai H, Minato N, Honjo T (1999) Development of lupus-like autoimmune diseases by disruption of the PD-1 gene encoding an ITIM motif-carrying immunoreceptor. Immunity 11:141–151. https://doi.org/10.1016/s1074-7613(00)80089-8
29. Okazaki T, Honjo T (2006) The PD-1-PD-L pathway in immunological tolerance. Trends Immunol 27:195–201. https://doi.org/10.1016/j.it.2006.02.001
30. Yin Y, Liu B, Cao Y et al (2022) Colorectal Cancer-Derived Small Extracellular Vesicles Promote Tumor Immune Evasion by Upregulating PD-L1 Expression in Tumor-Associated Macrophages. Adv Sci (Weinh) 9:2102620. https://doi.org/10.1002/advs.202102620
31. Pardoll DM (2012) The blockade of immune checkpoints in cancer immunotherapy. Nat Rev Cancer 12:252–264. https://doi.org/10.1038/nrc3239
32. Gilardini Montani MS, Falcinelli L, Santarelli R et al (2020) KSHV infection skews macrophage polarisation towards M2-like/TAM and activates Ire1 α-XBP1 axis up-regulating pro-tumorigenic cytokine release and PD-L1 expression. Br J Cancer 123:298–306. https://doi.org/10.1038/s41416-020-0872-0
33. Michikawa C, Gopalakrishnan V, Harrandah AM et al (2022) Fusobacterium is enriched in oral cancer and promotes induction of programmed death-ligand 1 (PD-L1). Neoplasia 31:100813. https://doi.org/10.1016/j.neo.2022.100813
34. Figueira EA, de Rezende ML, Torres SA, Garlet GP, Lara VS, Santos CF, Avila-Campos MJ, da Silva JS, Campanelli AP (2009) Inhibitory signals mediated by programmed death-1 are involved with T-cell function in chronic periodontitis. J Periodontol 80:1833–1844. https://doi.org/10.1902/jop.2009.090057
35. Liu X, Yang L, Tan X (2023) PD-1/PD-L1 pathway: A double-edged sword in periodontitis. Biomed Pharmacother 159:114215. https://doi.org/10.1016/j.biopha.2023.114215
36. Li W, Wu F, Zhao S, Shi P, Wang S, Cui D (2022) Correlation between PD-1/PD-L1 expression and polarization in tumor-associated macrophages: A key player in tumor immunotherapy. Cytokine Growth Factor Rev 67:49–57. https://doi.org/10.1016/j.cytogfr.2022.07.004
37. Arlauckas SP, Garris CS, Kohler RH et al (2017) In vivo imaging reveals a tumor-associated macrophage-mediated resistance pathway in anti-PD-1 therapy. Sci Transl Med. https://doi.org/10.1126/scitranslmed.aal3604
38. Francisco LM, Salinas VH, Brown KE, Vanguri VK, Freeman GJ, Kuchroo VK, Sharpe AH (2009) PD-L1 regulates the development, maintenance, and function of induced regulatory T cells. J Exp Med 206:3015–3029. https://doi.org/10.1084/jem.20090847
39. Peng RT, Sun Y, Zhou XD, Liu SY, Han Q, Cheng L, Peng X (2022) Treponema denticola Promotes OSCC Development via the TGF-β Signaling Pathway. J Dent Res 101:704–713. https://doi.org/10.1177/00220345211067401
40. Zhang C, Yue C, Herrmann A et al (2020) STAT3 Activation-Induced Fatty Acid Oxidation in CD8(+) T Effector Cells Is Critical for Obesity-Promoted Breast Tumor Growth. Cell Metab 31:148–61.e5. https://doi.org/10.1016/j.cmet.2019.10.013
41. Reck M, Rodríguez-Abreu D, Robinson AG et al (2016) Pembrolizumab versus Chemotherapy for PD-L1-Positive Non-Small-Cell Lung Cancer. N Engl J Med 375:1823–1833. https://doi.org/10.1056/NEJMoa1606774
42. Deng Y, Xia X, Zhao Y et al (2021) Glucocorticoid receptor regulates PD-L1 and MHC-I in pancreatic cancer cells to promote immune evasion and immunotherapy resistance. Nat Commun 12:7041. https://doi.org/10.1038/s41467-021-27349-7